RSC Advances

Journal Name

ARTICLE

"Lotus-effect" Tape: Imparting Superhydrophobicity to Solid Materials with Electrospun Janus Composite Mat

Received 00th January 20xx,
Accepted 00th January 20xx

DOI: 10.1039/x0xx00000x

www.rsc.org/

Bingbing Yue,[ac] Bowu Zhang,*[a] Jichun You,[b] Yongjin Li,[b] Linfan Li[a] and Jingye Li*[a]

To make superhydrophobic structure on materials surface is always an intricate and miscellaneous subject, which always requires special facility and techniques. Herein, a "lotus-effect" tape (LET) was designed to impart solid materials with superhydrophobicity as simple as taping. The so-called LET was prepared with Janus structure by dual-nozzle electrospinning, which consisted of lotus-effect upper layer and thermo-cohesive bottom layer. The LET can be pasted tightly on the surface of various substrates by ironing treatment with a household flatiron. The lotus effect property was endowed to substrates at the meanwhile. It is worth noting that the LET also can be detached easily from substrate involved, but without any damages to the original surface of substrate. This work provides a novel strategy to impart lotus-effect properties onto various materials beyond the limitation of special facility and techniques.

Introduction

Superhydrophobic surfaces can be found almost everywhere in nature,[1] in particular, the leaves of the lotus plant display an amazing self-cleaning effect, wherein water droplets can easily roll off and pick up dirt particles.[2,3] The secret of the so-called lotus effect lies in the low surface energy wax covering on the hierarchical micro/nanostructure of leaves, which allows air to be trapped, acting as a cushion for water droplets.[4,5] Inspired by the natural wisdom, various materials with lotus-effect surfaces, i.e. with a water contact angle (CA) greater than 150 ° and a sliding angle (SA) lower than 10 °,[6,7] have attracted considerable attentions from scientific and industrial communities. Many review papers have summarized various methods to fabricating the hierarchical micro/nanostructure on different materials and the possible approaches to reduce the surface energy.[8-13]

However, the current fabrication methods of lotus-effect surface depend on sometimes the surface structure of substrate, where the required hierarchical micro/nanostructure should be constructed on the smooth surfaces,[14-17] other times the chemical composition which low energy chemical agents should be deposited on the high surface energy materials.[18-21] These processes always require special facility and techniques, even skilled workers. To get rid of the limitation of facility and techniques is a new route worthy exploring to fabricate lotus-effect surface independent on the pristine surfaces chemical and physical properties of substrates. On the other hand, whereas many studies have concerned the fabrication and repair of the lotus-effect surface, not as many have investigated their removal.[22,23] Indeed, when the lotus-effect surface of materials is destroyed during practical use, it is hardly repaired under site conditions unless returning factory. If the destroyed lotus-effect surface on substrate can be replaced by a new surface easily at site, it would provide much convenience in practical use and broad the application of superhydrophobic materials or devices.

As we know, various kind of tapes are used in daily life, with a plastic or aluminium film as the upper layer and a bottom layer coated with a glue, which can be easily pasted onto the surface of different materials such as cardboard, wood, glass, metals, and so on. Inspired from this strategy, we plan to construct a "lotus-effect tape" (LET), which could be used to impart a lotus-effect surface on various materials by simple taping, and then be completely detached by simple treatment, releasing the pristine surfaces of the substrate, when the LET is destroyed in use. For the purpose, a Janus structure of the LET needs, which consisted of superhydrophobic upper layer and cohesive bottom layer.

Recently, various superhydrophobic materials with hierarchical micro/nanostructure prepared by electrospinning technique has been attractive[24] and applied in many fields, including membrane distillation,[25-27] biomaterial,[28] oil/water separation,[29-31] air filtrationt,[32,33] self-cleaning,[5,34,35] and so forth. For instance, X. Wang *et al* prepared a stable superhydrophobic organic/inorganic composite nanofibrous membranes for direct contact membrane distillation of saline water by electrospinning hydrophobic silica nanoparticles ($hSiO_2$ NPs) and poly(vinylidene fluoride) (PVDF) mixed colloids. Benefiting from the utilization of $hSiO_2$ NPs, the electrospun nanofibrous membranes were endowed with high porosity and superhydrophobic property, which resulted in excellent waterproofing and breathability.[25] While J. Lin *et al* demonstrated the surface of fibres prepared via electrospinning polystyrene solution

[a.] *CAS Center for Excellence on TMSR Energy System, Shanghai Institute of Applied Physics, Chinese Academy of Sciences, No. 2019 Jialuo Rd., Shanghai, 201800, People's Republic of China. E-mail: zhangbowu@foxmail.com, jingyeli@sinap.ac.cn; Tel.: +86-21-39194652, +86-21-39194505.*
[b.] *College of Material, Chemistry and Chemical Engineering, Hangzhou Normal University, No. 16 Xuelin Road, Hangzhou, 310036, People's Republic of China.*
[c.] *University of Chinese Academy of Sciences, Beijing, 100049, People's Republic of China.*

† Footnotes relating to the title and/or authors should appear here.
Electronic Supplementary Information (ESI) available: Picture of various liquid droplets sticking on electrospun PVDF mat surface; immersing as-prepared mats in saline solution and aqueous solution with different pH; contact angle of electrospun before and after chemical treatment; SEM images of concerned mats; pictures of water droplet rolling off from LET-covered glass slide and so on. See DOI: 10.1039/x0xx00000x

containing silica nanoparticles exhibiting a peculiar structure with the combination of nano protrusions and numerous grooves due to the rapid phase separation in electrospinning. The content of silica NPs incorporated into the fibre was proved as the key factor affecting the fibre surface morphology and hydrophobicity.[5]

Herein, we prepared a Janus composite mat consisted of lotus-effect upper layer and thermo-cohesive bottom layer. In which, a low surface energy polymer, poly(vinylidene fluoride) (PVDF), together with low surface energy nanoparticles consisting of fumed SiO_2 modified by hexamethyl disilazane (denoted as $mSiO_2$), were electrospun into $mSiO_2$@PVDF ultrafine fibres to fabricate the lotus-effect upper layer. However, the low surface energy of the electrospun mats also represents an obstacle for making tight cohesion with substrate by ordinary glue. In order to overcome this issue, we employed a dual-nozzle electrospinning process,[36, 37] in which poly(vinyl acetate) (PVAc), a thermo-cohesive and thermoplastic polymer with low softening and melting points (38 and 65 °C, respectively) ,[38, 39] was also electrospun into fibres and mixed with PVDF fibres to compose the bottom layer of composite mat. The resultant For with $mSiO_2$@PVDF upper layer and PVDF/PVAc bottom layer was pasted on to various substrates such as glass, paper, wood, plastics, and aluminium (Al) foil by ironing with a household flatiron. The micro-morphology and lotus effect property of Janus composite mats after ironing were investigated and the peel strength of Janus composite mats pasted on substrates, detaching process and recyclability were also carefully evaluated.

Experimental

Materials

Poly(vinylidene fluoride) (PVDF, Mw = 420,000) in powder form was purchased from Solvay Chemicals Co. (Belgium). Poly(vinyl acetate) (PVAc, M_W= 30,000~50,000), dimethyl formamide (DMF) and anhydrous alcohol were purchased from Sinopharm Chemical Reagent (China) Co., Ltd. Hexamethyl disilazane modified fumed silica ($mSiO_2$) (trade name TS530) was obtained from Cabot (China), Ltd. as a gift.

Fabrication of Janus composite mat

PVDF solution (10 g PVDF powder dissolved in 90 g of DMF, 10 wt%) was selected as precursor solution, and $mSiO_2$ was added at mass ratios ($mSiO_2$/PVDF) of 0, 0.5, 1.0, 1.5, and 2.0. The mixtures were stirred vigorously for 24 h at 60 °C for complete dispersion. PVAc solution (20 wt%) was prepared by dissolving 20 g of PVAc in 80 g of DMF. Here, PVDF, $mSiO_2$/PVDF and PVAc solution are the feed solution of subsequent electrospinning process. The setup of two-nozzle electrospinning process can be referred in our previous report.[37] The electrospun mats with Janus structure was prepared by following procedure. Firstly, PVAc and PVDF fibres were electrospun respectively from two different needles, which formed a bottom layer by interpenetrating PVAc and PVDF fibres as network, and then $mSiO_2$/PVDF fibres with different $mSiO_2$ contents was electrospun subsequently from the bottom layer surface, which services as the upper layer of the whole mat. The distance between the needle tip and top edge of drum was 15 cm; applied voltage was 12.5 kV; flow rate of all liquids was 0.4 $mL{\cdot}h^{-1}$ and both bottom and upper layer were electroeffect surface

Analyses

The surface morphology of the Janus composite mats were observed by a field-emission scanning electron microscope (FESEM, Hitachi S-4800, Japan). The samples were sputter-coated with 10 nm gold layer and examined at an acceleration voltage of 10 kV. Three-dimensional morphology of fibres were obtained by atomic force microscope (AFM, E-Sweep, Seiko Instruments Inc., Japan) in taping mode. Contact angles (CAs) were measured on an Attension Theta system (KSV Instruments Ltd., Finland), with a volume of 5 μl deionized water. The average value of five measurements performed at different positions on the same sample was adopted as the contact angle. The inclination angles of samples were gradually increased until the water droplets rolled down, then the sliding angles (SAs) were obtained. The bond strength of the Janus composite mats on substrates were tested by a 90 ° peel strength testing machine (MK-BL-X90, MaiKe Instruments Ltd., China). The chemical stability of the Janus composite mats were also tested. The mats were completely soaked in aqueous solution with different pH (prepared with HCl or NaOH) and saturated saline (NaCl) aqueous solution for 12h. And the contact angles were measured after washing and drying.

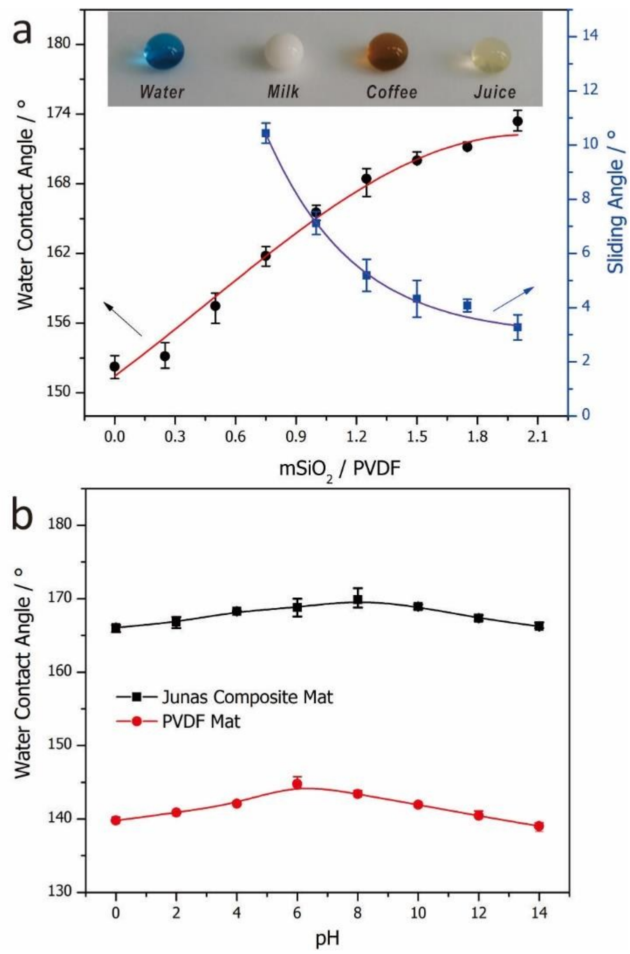

Fig.1 (a) Water contact angles and sliding angles of electrospun Janus composite mats with different mass ratio of $mSiO_2$/PVDF in upper layer fibres; the insert is a digital picture of different liquid droplets on the Janus composite mat (mass ratio: 1.5). (b) The stability of Janus composite mat (mass ratio: 1.5) and PVDF mat in aqueous solution with different pH.

Results and discussion

Fig. 1a depicts that no matter how much the mass ratio of $mSiO_2$/PVDF in upper layer fibres of Janus composite mats, the water contact angles (CAs) are all in excess of 150°, and increased as the mass ratio increasing gradually. We also find the droplets of some common liquids, including milk, orange juice and coffee can stand on the surface of mats as almost perfect ball (see the insert of **Fig. 1a**). Interestingly, the sliding angles (SAs) of water droplets on mats are decreased monotonously as the mass ratio increasing and when the mass ratio up to 1.0, the SAs of mats come to 10 ° less, which exhibits lotus effect of superhydrophobic behaviour. While water droplets, as well as milk, orange juice and coffee, stuck firmly to the mat even when it was turned upside vertically even down (Fig. S1), although the CA of water droplets on the PVDF mat reached 155 °. It indicates the surface of PVDF mat corresponds to "rose petal effect" of superhydrophilic behaviour, in which the surface has strong adhesion to water,[18, 40] and a mat with lotus-like surface can be prepared by introducing $mSiO_2$ NPs ratio in the fibres of upper layer.

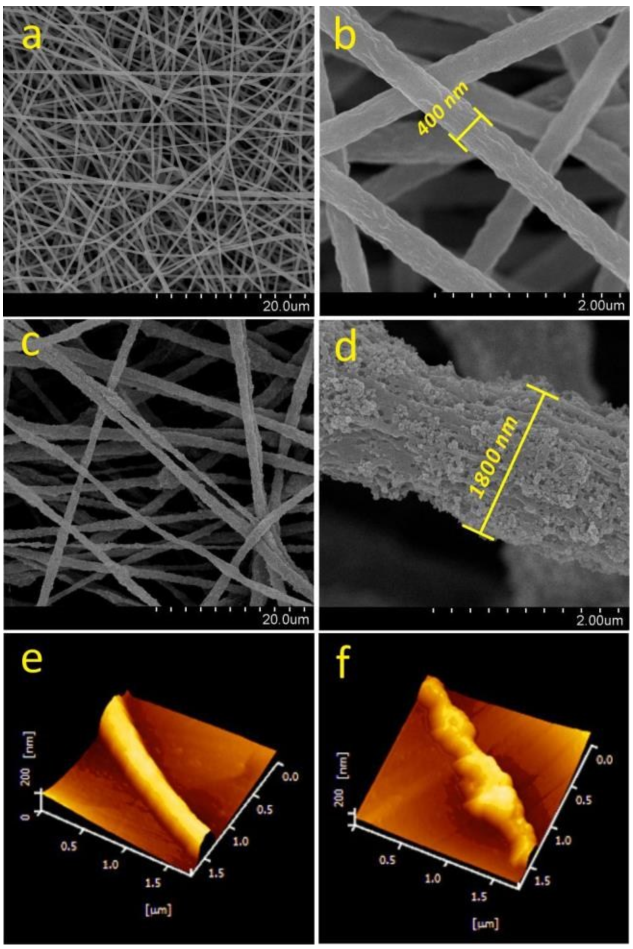

Fig. 2 SEM images of upper layers of electrospun PVDF mat (a, b) and Janus composite mat with 1.0 of mass ratio of $mSiO_2$/PVDF in upper layer fibres (c, d). AFM 3D images of fibre in PVDF mats (e) and (f) upper layer of Janus composite mat (mass ratio: 1.5).

In order to evaluate chemical stability of Janus composite mats, we immersed the mats completely in aqueous solutions with different pH and saturated saline solution as the way shown in **Fig. S2**. As **Fig. 1b** shows, after immersion in strong acid (pH=0) or alkaline (pH=14), the CAs of Janus composite mats were decreased about 5 ° in comparison to that before immersion (ca. 170 °), but still much higher than 150 °. In contrast, the degree of CAs decreasing of PVDF mats reached around 10 °, but the CAs of PVDF mats after strong acid and alkaline immersion got beneath 140 °. The same trends were also found from the results of saline solution immersion (**Fig. S3**). This indicates that introducing $mSiO_2$ into PVDF fibre is helpful to enhance the chemical stability of composite mats.

Generally, the microstructural morphology of materials plays a very important role to materials surface wettability, and the hierarchical micro/nanostructure is an indispensable feature of materials constructed with lotus effect surface.[3] Here, we investigated the micromorphology of obtained electrospun composite mats through field emission scanning electron microscopy (FE-SEM). As **Fig. 2a&b** shows, PVDF mat is a web of PVDF fibres of smooth appearance and with uniform diameter, around 400 nm. After introducing $mSiO_2$ NPs in PVDF fibres, the fibres became more and more rough as the content of $mSiO_2$ NPs (mass ratio) increasing (**Fig. 2c&d**, **Fig. S4a-f**). **Fig. 2d** shows that there're many nano-protrusions and numerous grooves pervading over the $mSiO_2$@PVDF fibres surface, which formed during the rapid phase separation in electrospinning $mSiO_2$/PVDF mixture solution.[5] When the mass ratio at 0.5, some spindle-like knots and roe-like aggregates embed in the line of $mSiO_2$/PVDF fibres, diameter of some fibres was increased to 1000 nm (**Fig. S4a&b**). These $mSiO_2$/PVDF fibres was further thicken to about 1800 nm of diameter until adding $mSiO_2$ to 1.0 of mass ratio, and the fibres exhibited more uniform diameter and no spindle-like knots appearance (**Fig. 2c&d**). It could be reasoned that mixing $mSiO_2$ NPs into the PVDF solution has increased the non-volatile ingredient and reduced the fluidity of mixture solution (due to the excessively high surface area of $mSiO_2$ NPs), which results in the diameters of fibres thicker. When the mass ratio increasing to 1.5 and 2.0, the fibres got more and more defects and uneven thickness, some big agglomerates scattered in the composite mats (**Fig. S4c-f**). It is accountable that the fluidity of mixture solution was reduced dramatically by overmuch $mSiO_2$ NPs introducing, which leads to the electrospun jets unstable and intermittent. However, the surface of fibres are completely covered with nano-protrusions, which is the reason that SAs of Janus composite mats are lower than 10°.

Furthermore, we also used an atomic force microscopy (AFM) to observe the hierarchical micro/nano structure of Janus composite mats surface. As the AFM 3D images of fibre in PVDF mats (**Fig. 2e**) and upper layer of Janus composite mat (**Fig. 2f**) shows, it is apparent contrast with the uniform thickness and smooth surface of pure PVDF fibre, while the as-prepared $mSiO_2$@PVDF fibre shows marked fluctuations on the surface, which is due to the accumulation of $mSiO_2$ NPs undulating surface of fibres.

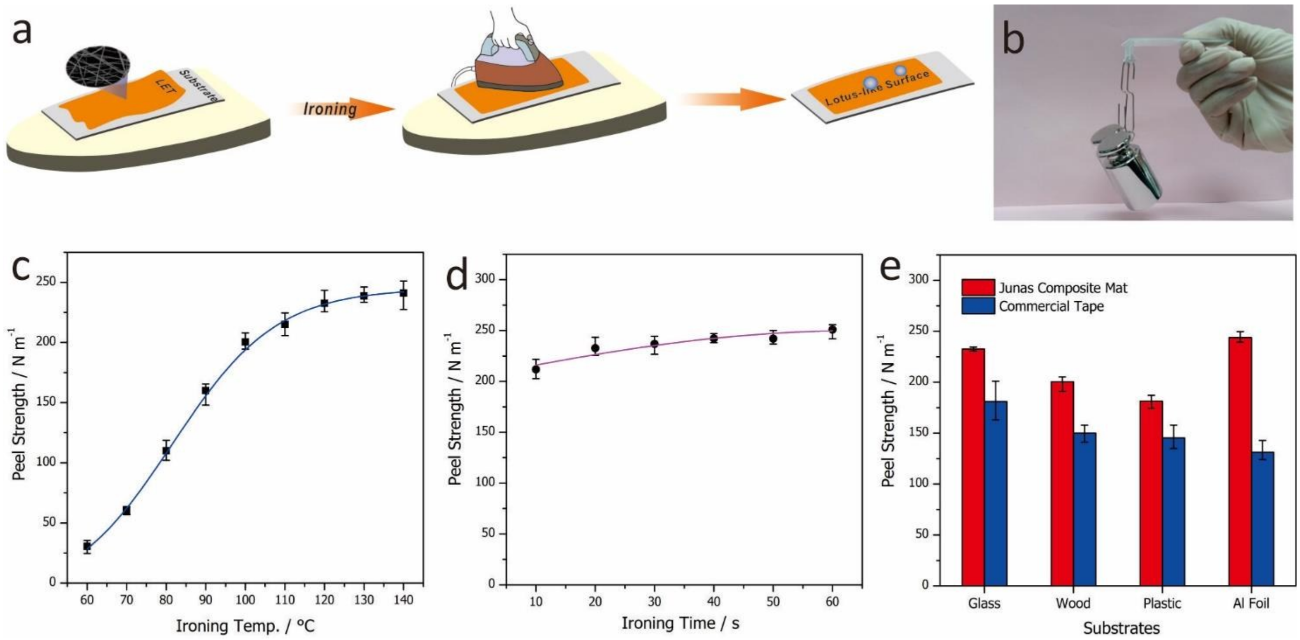

Fig.3 (a) Illustration of the process impart substrates lotus-like surface with Janus composite mat (mass ratio: 1.5) by ironing treatment; (b) Demonstration of the high peel strength of Janus composite mat (mass ratio: 1.5), performed by hanging two 200 g weights; The effect of (c) temperature and (d) duration of ironing treatment to the peel strength of Janus composite mat (mass ratio: 1.5) pasted on glass slide; (e) Comparison of the peel strength of Janus composite mat (mass ratio: 1.5) and commercial tape pasted on different substrates.

As mentioned above, the Janus composite mat here is consisted of upper layer prepared by electrospinning $mSiO_2$/PVDF mixture solution and bottom layer obtained by dual-nozzle electrospinning PVDF and PVAc solution, respectively. The SEM image of bottom layer (Fig. **S5**) shows the micromorphology of fibres in bottom layer are thinner and smooth, very different from that of upper layer, which clearly confirms the Janus structure of composite mats, but no only the chemical composition difference between upper layer and bottom layer. In consideration that PVAc is thermo cohesive and effective constituent of organic glues, we designed a simple approach to attach Janus composite mat onto substrate as illustrated in **Fig. 3a**. In which, the Janus composite mat were laid on a substrate, such as glass slide, wood and paper, then ironed by a household flatiron under about 3.6 kPa pressure, pre set temperature and duration. After 120 °C and 30 s ironing treatment, the Janus composite mat was tightly pasted on a glass slide and cannot be peeled off even two 200 g weights were hanged on the end of mat (Fig. **3b**). Moreover, the water droplets easily rolled off from the surface of Janus composite mat pasted glass slide, which was laid on floor with about 5° of inclination angle (**Fig. S6**). It demonstrates the lotus-like surface can be effectively imparted to substrates by ironing treatment with Janus composite mat. In other words, the Janus composite mat works as a "lotus-effect" tape (LET) to allocate lotus-like surface on substrates. For brevity, the Janus composite mat afterward is expressed as LET instead.

The strength of LET pasted substrate was measured by means of peel strength tests in the direction 90 °. **Fig. 3c** and **3d** show the influence of ironing temperature and duration on peel strength of LET from glass slide. It can be found the peel strengths shows a strong dependence on the ironing temperature, which the high ironing temperature results in high peel strengths (**Fig. 3c**). While the duration of ironing treatment is relatively short effect on peel strength, and the maximum can be obtained about 30 s (**Fig. 3d**). It means LET can be rapidly (just within 60 s duration) pasted onto substrates by ironing treatment, which is a good signal for practical usage. The optimized conditions for ironing treatment of the LET on a glass substrate is at 120 °C for 30 s, which leads to a resulting peel strength of up to 232 $N \cdot m^{-1}$. This strength is equivalent to saying that a 2.5 cm width of LET pasted on glass could withstand a weight of 580 g in the vertical direction, which was demonstrated using two 200 g weights, as shown in **Fig. 3b**. As a comparison, PVAc glue was previously coated on surface of glass and unitary $mSiO_2$@PVDF electrospun mat, after them dried, then ironed at 120 °C for 30 s. But the resulting peel strength was only 57.5 $N \cdot m^{-1}$, much lower than that of the LET. Moreover, the peel strength of the LET was compared with that of commercial tape attached on glass, wood, plastic, and aluminium (Al) foil, and the results show that the interactions between LET and substrate after ironing treatment are much stronger than those measured for the commercial tape pasted at room temperature (**Fig. 3e**).

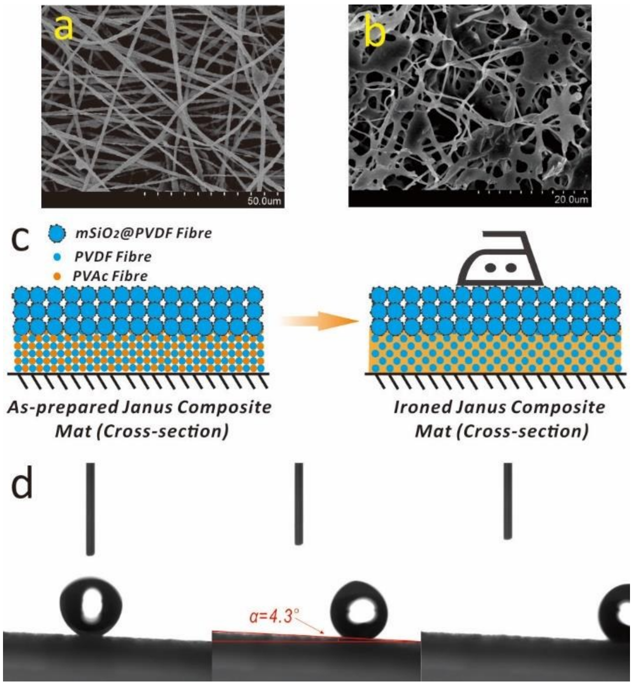

Fig. 4 SEM images of the (a) upper and (b) bottom layer of the Janus composite mat (mass ratio: 1.0) after ironing treatment at 120 °C for 30 s. (c) The schematic program of Janus composite mats were pasted onto substrates by ironing treatment. (d) The lotus effect on glass slide pasted with Janus composite mat (mass ratio: 1.5)

The ironed LET was peeled off from glass slide and its upper and bottom layer were characterized by FE-SEM. Fig. **4a** shows the micro-morphology of upper layer is almost no changes comparing with that of before ironing (**Fig. 2c**). That is because the melt point (ca. 175 °C) of PVDF is much higher than the ironing temperature (120 °C), the $mSiO_2$@PVDF fibre in upper layer can withstand and keep its shape in the ironing process. But after ironing treatment, some fibres in the bottom layer were transformed to melt lump, the others still kept fibre form and were stuck together by melt lump (**Fig. 4b**), which is much different to the pristine bottom layer (**Fig. S5**). The reason can be illustrated by **Fig. 4c.** As described previously, the bottom layer is consisted of PVDF fibre and PVAc fibre. The PVAc fibre can be melt at the ironing temperature due to its melt point (ca. 65 °C) much lower than ironing temperature. The melt PVAc fibres turn to a semi continuous phase, glues PVDF fibres and substrate together tightly, which contributes to the high peel strength of LET with substrates.

It is particularly gratifying that the lotus-effect properties of LETs were retained after pasted onto glass slides by ironing treatment. As **Fig. 4d** shows, the water droplet can roll off rapidly from the surface of LET-covered glass slide that laid with about 4.3 ° of inclination angle, which is similar to that of LET before ironing treatment (**Fig. 1a**). Dust particles, such as carbon black, can be easily carried off from the LET covered glass slide by the rolling water droplets (**Fig. S7**). Those would thank the hierarchical microstructure of $mSiO_2$@PVDF fibres in upper layer of LET were not damaged in the ironing process. Therefore, LET coupling with ironing treatment is a simple way to impart lotus effect properties to substrate surfaces. Furthermore, the LET can also be applied onto soft substrates such as paper. A water droplet on the LET-covered area of printed paper can roll over freely (**video S1** in **ESI**), which means the lotus effect property has been imparted onto the surface of paper.

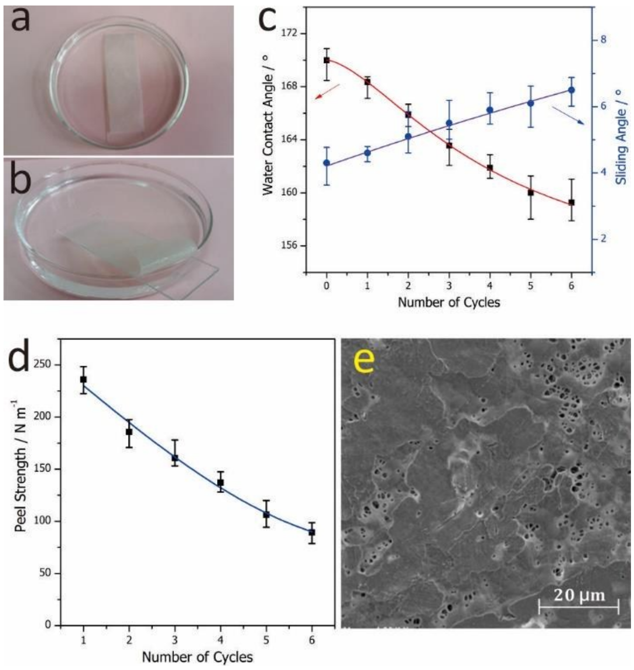

Fig.5 (a) Soaking of LET-pasted glass slide in ethanol for 30 s. (b) Detaching LET from glass slide after soaking in ethanol. (c) The CA and SA of LET-covered glass slides prepared with detached LET. (d) Peel strength of LET-covered glass slides prepared with detached LET. (e) SEM image of the bottom layer of the LET after 5 reusing cycles.

As far as we know, the superhydrophobic structure constructed on substrates by conventional methods are almost disposable, and it is very difficult to be refreshed without damage to the substrates. But then, this problem is not a handicap yet for the LET. As it shown in **Fig. 5a** and **5b**, the LET covered glass slide was soaked in ethanol at room temperature for 30 s, and the LET can be detached easily and completely from glass slide, but without any damages. It is owning to that alcohol is able to swell PVAc and reduce the surface adhesion energy of PVAc and glass slide (**Fig. 4c**), which results in exfoliation of the LET.

In consideration that PVAc still exists within the bottom layer of LET, the recyclability of detached LET was tested by repeating the process of ironing and alcohol exfoliation. Fig. **5c** shows the CA of LET covered glass slide is decreased, and SA is increased slightly as recycling times increasing After recycling 6 times, the CA decreases to around 157 °, SA increases to 6.5 °, which indicates the lotus effect of LET is still retained after multi-time recycling. It also can be confirmed by the SEM image of upper layer of the LET after 5 recycling times (**Fig. S8**), which shows the morphology of the nano-protuberances that compose the hierarchical network structure is retained, keeping almost the same appearance as in the as-prepared sample shown in Fig. **S4d**. However, the peel strength of LET-covered glass slides prepared with detached LET obviously decreased, and after 5 recycling times it reached a value less than half that of the fresh LET, and close to the corresponding value of the coated PVAc (Fig. **5d**). The SEM image of the bottom layer of LET after 5 reusing cycles, presented in Fig. **5e**, shows that PVAc appears mainly as a film attached to the bottom layer, which means that most PVAc in bottom layer was deposited from the network of fibres, due to the repeated melting processes. Therefore, the LET can be reused 5 times at least to build up lotus effect surface on substrates after preparation.

Fig. 6 (a) A LET-covered paper with a printed logos of SINAP (Shanghai Institute of Applied Physics, Chinese Academy of Sciences). (b) After spraying alcohol on the back of LET-pasted paper. (c) The restored paper and LET after detaching.

The recycling experiment on smooth and rigid surface of glass slide may be not able to comprehensively evidence the gentleness of detaching process. A LET-covered paper was prepared by ironing treatment (Fig. 6a), subsequently, some alcohol was sprayed on the back of LET-covered paper (**Fig. 6b**). The LET was completely detached from paper and the ink-printed logo in the centre marked with green rectangle was still clear (**Fig. 6c**), even though some patterns in the top and bottom sides appeared blurred as pointed out due to the soakage from the water droplets. This confirms that the detaching procedure using alcohol causes only minimal damage to various substrates surface, even the soft and vulnerable substrates.

Conclusions

In conclusion, a Janus composite mat with a lotus effect upper layer and thermo-cohesive bottom layer was designed and it is really able to impart its lotus effect property onto substrates as simple as taping assisted by ironing. The hierarchical microstructure of $mSiO_2$ embed PVDF fibres network contributes to lotus effect property of upper layer, and PVDF and PVAc fibres blending network prepared by dual-nozzle electrospinning allocates the ability of thermos-cohesion to the bottom layer. In this manuscript, we showed that the Janus composite mat can be pasted on various substrates surface tightly and impart its lotus effect property onto substrates easily by ironing process. Interestingly, the LET can be easily detached from substrate by soaking or spaying with alcohol, but brings almost no damages to the surface of substrate, no matter whether it is smooth and rigid or rough and soft substrate. Furthermore, the detached LET can be reused at least 5 times to build up lotus effect surface on substrate by simply repeating the ironing process. All in all, the approach reported here definitely provides a novel strategy to impart lotus effect properties to various substrates beyond the limitation of special facility and techniques.

Acknowledgements

This work was financially supported by National Natural Science Foundation of China (Grants No. 51473183, 11305248 and 11475246), and the "Strategic Priority Research Program" of the Chinese Academy of Sciences (Grant No. XDA02030200). We appreciate sincerely Cabot (China), Ltd. for the kindly supply of $mSiO_2$ NPs as a gift.

Notes and references

‡ Footnotes relating to the main text should appear here. These might include comments relevant to but not central to the matter under discussion, limited experimental and spectral data, and crystallographic data.

1. L. Feng, S. Li, Y. Li, H. Li, L. Zhang, J. Zhai, Y. Song, B. Liu, L. Jiang and D. Zhu, *Adv. Mater.*, 2002, **14**, 1857-1860.
2. T. Sun, L. Feng, X. Gao and L. Jiang, *Acc. Chem. Res.*, 2005, **38**, 644-652.
3. B. Bhushan and Y. C. Jung, *Prog. Mater. Sci.*, 2011, **56**, 1-108.
4. Q. X. Zhang, Y. X. Chen, Z. Guo, H.-L. Liu, D. P. Wang and X. J. Huang, *ACS Appl. Mater. Interfaces*, 2013, **5**, 10633-10642.
5. J. Lin, Y. Cai, X. Wang, B. Ding, J. Yu and M. Wang, *Nanoscale*, 2011, **3**, 1258-1262.
6. L. Yin, Y. Wang, J. Ding, Q. Wang and Q. Chen, *Appl. Surf. Sci.*, 2012, **258**, 4063-4068.
7. S. Wang, Y. Li, X. Fei, M. Sun, C. Zhang, Y. Li, Q. Yang and X. Hong, *J. Colloid Interface Sci.*, 2011, **359**, 380-388.
8. I. Sas, R. E. Gorga, J. A. Joines and K. A. Thoney, *J. Colloid Interface Sci.*, 2012, **50**, 824-845.
9. B. Bhushan, *Phil. Trans. Roy. Soc. A*, 2009, **367**, 1445-1486.
10. T. Verho, C. Bower, P. Andrew, S. Franssila, O. Ikkala and R. H. A. Ras, *Adv. Mater.*, 2011, **23**, 673-678.
11. V. A. Ganesh, H. K. Raut, A. S. Nair and S. Ramakrishna, *J. Mater. Chem.*, 2011, **21**, 16304-16322.
12. Y. Y. Yan, N. Gao and W. Barthlott, *Adv. Colloid Interface Sci.*, 2011, **169**, 80-105.
13. S. Wang, K. Liu, X. Yao and L. Jiang, *Chemical Reviews*, 2015, **115**, 8230-8293.
14. B. Zhang, L. Liu, S. Xie, F. Shen, H. Yan, H. Wu, Y. Wan, M. Yu, H. Ma, L. Li and J. Li, *RSC Adv.*, 2014, **4**, 16561-16566.
15. S. Y. Lee, Y. Rahmawan and S. Yang, *ACS Appl. Mater. Interfaces*, 2015, **7**, 24197-24203.
16. Y. Wu, T. Hang, J. Komadina, H. Ling and M. Li, *Nanoscale*, 2014, **6**, 9720-9726.

17. C. Hao, J. Li, Y. Liu, X. Zhou, Y. Liu, R. Liu, L. Che, W. Zhou, D. Sun, L. Li, L. Xu and Z. Wang, *Nat. Commun.*, 2015, **6**, 7986.
18. Z. Cheng, M. Du, H. Lai, N. Zhang and K. Sun, *Nanoscale*, 2013, **5**, 2776-2783.
19. B. Deng, R. Cai, Y. Yu, H. Jiang, C. Wang, J. Li, L. Li, M. Yu, J. Li, L. Xie, Q. Huang and C. Fan, *Adv. Mater.*, 2010, **22**, 5473-5477.
20. J. Wu, J. Li, B. Deng, H. Jiang, Z. Wang, M. Yu, L. Li, C. Xing and Y. Li, *Sci. Rep.*, 2013, **3**.
21. J. Wu, J. Li, Z. Wang, M. Yu, H. Jiang, L. Li and B. Zhang, *RSC Adv.*, 2015, **5**, 27752-27758.
22. P. Kim, M. J. Kreder, J. Alvarenga and J. Aizenberg, *Nano lett.*, 2013, **13**, 1793-1799.
23. K. Chen, S. Zhou and L. Wu, *Chem. Comm.*, 2014, **50**, 11891-11894.
24. J. Wu, N. Wang, Y. Zhao and L. Jiang, *J. Mater. Chem. A*, 2013, **1**, 7290-7305.
25. X. Li, X. Yu, C. Cheng, L. Deng, M. Wang and X. Wang, *ACS Appl. Mater. Interfaces*, 2015, **7**, 21919-21930.
26. Z. Q. Dong, X.-H. Ma, Z.-L. Xu and Z.-Y. Gu, *RSC Adv.*, 2015, **5**, 67962-67970.
27. Z.-Q. Dong, B. J. Wang, X. h. Ma, Y. M. Wei and Z. L. Xu, *ACS Appl. Mater. Interfaces*, 2015, **7**, 22652-22659.
28. H. Y. Li, Y.-Y. Lee, Y. Chang, C. H. Lin and Y.-L. Liu, *Adv. Mater. Interfaces*, 2015, **2**, 1500065.
29. X. Tang, Y. Si, J. Ge, B. Ding, L. Liu, G. Zheng, W. Luo and J. Yu, *Nanoscale*, 2013, **5**, 11657-11664.
30. Y. Si, Q. Fu, X. Wang, J. Zhu, J. Yu, G. Sun and B. Ding, *ACS Nano*, 2015, **9**, 3791-3799.
31. Y. Shang, Y. Si, A. Raza, L. Yang, X. Mao, B. Ding and J. Yu, *Nanoscale*, 2012, **4**, 7847-7854.
32. H. Wan, N. Wang, J. Yang, Y. Si, K. Chen, B. Ding, G. Sun, M. El-Newehy, S. S. Al-Deyab and J. Yu, *J. Colloid Interface Sci.*, 2014, **417**, 18-26.
33. N. Wang, Z. Zhu, J. Sheng, S. S. Al-Deyab, J. Yu and B. Ding, *J. Colloid Interface Sci.*, 2014, **428**, 41-48.
34. P. Ragesh, S. V. Nair and A. S. Nair, *RSC Adv.*, 2014, 4, 38498-38504.
35. J. H. Kong, T. H. Kim, J. H. Kim, J. K. Park, D. W. Lee, S.-H. Kim and J. M. Kim, *Nanoscale*, 2014, **6**, 1453-1461.
36. C. Zhang, Y. Li, W. Wang, N. Zhan, N. Xiao, S. Wang, Y. Li and Q. Yang, *Eur. Polym. J.*, 2011, **47**, 2228-2233.
37. S. Xie, X. Liu, B. Zhang, H. Ma, C. Ling, M. Yu, L. Li and J. Li, *J. Mater. Chem. A*, 2015, **3**, 2552-2558.
38. C. M. Roland and R. Casalini, *Macromolecules*, 2003, **36**, 1361-1367.
39. G. A. G. Novoa, J. Heinämäki, S. Mirza, O. Antikainen, A. I. Colarte, A. S. Paz and J. Yliruusi, *Eur. J. Phar. Biophar.*, 2005, **59**, 343-350.
40. L. Feng, Y. Zhang, J. Xi, Y. Zhu, N. Wang, F. Xia and L. Jiang, *Langmuir*, 2008, **24**, 4114-4119.

Table of Contents

Lotus-effect tape: superhydrophobic surface was easily constructed by thermally taping an electrospun Janus composite mat on various substrates.

Graphic Abstract